RSC Advances

ROYAL SOCIETY
OF CHEMISTRY

www.rsc.org/advances

Tuning the band gap and optical properties of γ-Si_3N_4 with rare earth element Ce

Yan-Xiao Han[a], Chuan-Lu Yang[a*], Mei-Shan Wang[a], Xiao-Guang Ma[a]

Abstract

The present paper reports the investigation of optoelectronic properties of doped γ-Si_3N_4. The rare earth element Ce is used as dopant. Two structures are picked out from the four ones in different doping methods by comparing their formation and binding energies. The effects of doping methods and concentrations are explored based on the favourable structures. Four cases with different concentrations are considered for each doping method. Their electronic and optical properties are calculated on the basis of hybrid density functional theory with Hubbard U correction. The Ce dopant with the proper doping method and concentration results in the decreased band gaps, improved low-energy electron transition and enhanced absorption in the range of solar energy. The mechanism for the doping effect is elucidated by analyzing the electronic structure.

Keywords: optical properties; semiconductor; optoelectronic materials; dielectric properties

1. Introduction

Silicon nitride (Si_3N_4) is an important engineering ceramic material owing to its superior mechanical properties, high chemical and thermal stability, and good wear resistance. It has been widely applied for cutting tools, engines components, ball bearings and gas turbines. [1-3] The α-Si_3N_4 and β-Si_3N_4 can be obtained under conventional synthetic conditions. Both phases are in the hexagonal crystal system. In 1999, the cubic spinel structure (γ-Si_3N_4) was synthesized by applying high pressure with high temperature. [4] An *ab initio* density functional theory (DFT) calculation suggested that γ-Si_3N_4 has a direct band gap of 3.45 eV. [5] This is in contrast to the

---

[a] School of Physics and Optoelectronic Engineering, Ludong University, Yantai 264025, China

[*] Corresponding author. Tel: +86 535 6672870. E-mail address: scuycl@gmail.com. (C.L. Yang).

band gaps of α and β-Si_3N_4 whose are wider and indirect. The hardness of γ-Si_3N_4 can be compared to stishovite, and also is increased in comparison to β-Si_3N_4. Because of the unique combination of mechanical and electronic properties, γ-Si_3N_4 is candidate for optoelectronic applications including UV LEDs and lasers. [6] Studies have been carried out to examine the electric and optical properties of γ-Si_3N_4.[7-9] But further characteristics are necessary to allow these materials to become as widely used as their hexagonal predecessors. As an efficient photoelectric material, γ-Si_3N_4 must have optimal band gap and absorption coefficient in the range of solar light. However, the band gap of γ-Si_3N_4 is too wide, and the optical absorption is too small to effectively convert solar energy. The method of doping is used to improve the electronic and optical properties. [10-12] Moreover, it is necessary to find effective dopant and relevant doping method to get a new doped material. The material should have reduced band gap and enhanced absorption coefficient, but do not have holes and intraband transition. Rare earth element Ce ($4f^1 5d^1 6s^2$) with vacant and uneasily ionized d and f electrons is possible to be effective dopant. Because it is relatively uneasy to introduce holes, and also is used as luminescence center. [13-18] Recently, the luminescence proerties of α-Si_3N_4 activated by Ce have been studied, and the blue light emitting was found. [19] The study encourages us to explore the optical properties of γ-Si_3N_4 caused by Ce dopant. We investigate the way of decreasing the band gap and increasing the adsorption of γ-Si_3N_4 with dopant Ce using the hybrid DFT and Hubbard U correction. Moreover, the doping site and concentration are emphasized. We also explored the mechanisms with electronic structure calculations to provide fully understanding of the doping effect.

2. Computational models and methods

Figure 1 shows the modules of doped γ-Si_3N_4. It can be seen from the cubic spinel form that Si atoms occupy both tetrahedral (tet) and octahedral (oct) sites, but N atoms only occupy tet sites. When the Ce atom is doped, both substitutional and interstitial sites are possible doping sites. It depends on the synthesis conditions. Ce@Si-T, Ce@Si-O and Ce@N are used to stand for the doping method of one Ce atom substituting tet Si, oct Si and N atom, respectively. For the interstitial site of Ce atom, the possible positions are enormous. Here we just list one of them (Ce-IN). The formation energy (E_f) which is calculated at the two extreme conditions, i.e., the Si-rich limit and the N-rich limit, is given as a function of the atomic chemical potentials and Fermi energy: $E_f(q) = E_T(q) - n_{Si}\mu_{Si} - n_N\mu_N - \mu_x + qE_F$.[1, 2] The E_T is the total energy of a supercell containing an impurity atom; n_{Si} and n_N represent the number of Si and N atoms, respectively; μ_{Si}, μ_N and μ_x are the chemical potential of Si, N, and the impurity atoms, respectively; and E_F is the Fermi energy. The bind energy (E_b) of the crystal, which is given as a function of total energy and the total sums of free energies, represents its energy stability. [12] So the most suitable doping method of Ce dopant is suggested in terms of E_f and E_b, which are calculated with the model of the 56-atom supercell (2×2×2). Then the influences of concentration on the electronic and optical properties are investigated based on the most suitable doping models. All the doping concentration in this paper refers to atomic ration. There are five equivalent tet Si atoms in the supercell, excluding the ones on the side of cell. When one Ce atom replaces one tet Si atom labeled as Ce@Si-T-I, the concentration is 0.042. The number of Ce atom is added to get higher doping concentrations which are 0.083, 0.125, and 0.167. The corresponding cases are labeled as Ce@Si-T-II, Ce@Si-T-III and Ce@Si-T-IV, respectively. In order to avoid the influence of interaction among multiple Ce atoms, the doped atoms are equally distributed in the models, and the distance between every two Ce atoms is about 5.6 Å. As for the Ce@Si-O cases, different concentrations are labeled as Ce@Si-O-I, Ce@Si-O-II, Ce@Si-O-III and Ce@Si-O-IV, respectively. The calculation are conducted by a first-principles plane-wave pseudo-potential (PWP), using the CASTEP procedure of Materials Studio 6.0. [20] The optimized structures are obtained via DFT calculations with the functional of GGA of PBE form. All the calculated electronic and optical properties are obtained with the use of the B3LYP hybrid functional. The Norm-conserving pseudopotential is used in all the calculations of properties. The cutoff energy is chosen from the three tested values which are 350, 400 and 450 eV, respectively. The energy level of 400 eV which corresponds a 3×3 ×3 Monkhorst-pack set of K-points is effective to get the convergent result. Different numbers of empty bands (20, 30, 40 and 50) are also tested in which the number of 40 is enough to get the right band structure. Because of the existence of 4f-electrons, we consider B3LYP+U method in the Ce doped cases. To get the accurate Hubbard U value of Ce-4f electrons, different values of U ranging from 6 to 16 eV are used. The Ce@Si-T-IV with good symmety is set as the testing module. We choose the value of 10 eV which can obtain the maximal band gap value for the Ce doped cases. The band gap value depending on the U value is shown in Figure 2. Convergence criteria in energy, force stress, and displacement are set as 2×10^{-5} eV, 0.05 eV/Å, 0.1GPa and 0.002 Å, respectively. The electronic structures and optical properties are calculated with the corresponding optimized crystal geometries. Optical properties of material can be measured from the complex dielectric function which consists of real part ε_1 and imaginary part ε_2, in which the real part can be calculated using Kramers-Krönig transformation. All other optical constants, such as the dielectric function, absorption coefficient and conductivity are derived from ε_1 and ε_2, while the transmissivity is calculated with the method related in Ref. 21.

3. **Results and discussions**

3.1. Calculated structure properties of doped γ-Si_3N_4

In terms of the E_b and E_f, we first find the most suitable doping method for Ce dopant. If its E_b is minus, the doped cases are identified to be stable in energy. [12] The minus E_f with the bigger absolute value means that the formation of the doped case is possible. Table 1 show that both Ce@Si-T and Ce@Si-O have minus E_bs and E_fs. Moreover, the absolute value of E_b of Ce@Si-T is about 2.3 eV bigger than that of Ce@Si-O, and the absolute value of E_f is also bigger than those of Ce@Si-O in both Si rich and N rich condition. It indicates that Ce@Si-T is more stable than Ce@Si-O, and the Ce atom is more inclined to occupy tet Si sites. Because of the quite small absolute values of E_b and the positive values of E_f, Ce@N and Ce-IN methods are not suitable for doping. Therefore we omit the analysis of those cases. By comparing the lattice parameter and average bond length with those of intrinsic γ-Si_3N_4, we find that doping Ce results only slight change. This implies that doping Ce has not caused lattice distortion. So we concentrate on the methods of Ce@Si-T and Ce@Si-O to study the influence of doping concentration on the electronic and optical properties of doped γ-Si_3N_4.

3.2. Electronic properties of doped γ-Si_3N_4

3.2.1. Electronic properties of Ce@Si-T cases

According to the analysis of E_f and E_b, We have found that Ce@Si-T is a favorable doping method. However, the influence of Ce concentration on the electronic and optical properties of γ-Si_3N_4 should be considered. Figure 3 shows the density of states (DOS) and band structure of intrinsic γ-Si_3N_4. The calculated direct band gap is 5.023 eV, which is accord with the recent experimental value 4.85 eV [5] and 4.8eV [6], and better than other theoretical values 3.45 eV [5], 3.00 eV [10] and 3.58 eV [12] in the literature. For intrinsic γ-Si_3N_4, the valence band (VB) originates mainly from N-2p orbitals, while the lowest conduction band is composed of Si orbitals. Figure 4 shows the DOS and band structures of cases derived from Ce@Si-T with different doping concentrations. The shape of highest VB shows apparent change compared with intrinsic γ-Si_3N_4, meanwhile the Ce-5d orbitals and Ce-4f orbitals add to the composition of the highest VB. For Ce@Si-T-I, the conduction band (CB) composed of the Si orbitals and few Ce orbitals reduces to 4.6 eV, which is reduced by 0.4 eV compared with the CB of intrinsic γ-Si_3N_4. Meanwhile, a new occupied band composed of N-2p and Ce-5d orbitals appears, which is below the Fermi energy at around -0.2 eV. Because of the interaction among the electronic charges which produces Multi-body effect or the overlap of impurities and defect band，the band gap narrows down to 4.069 eV. With the increase of Ce concentration, the interaction among the electronic charges gets enhanced. For Ce@Si-T-II, the location of the CB reduces about 1.3 eV, which further decreases the band gap. With the further increase of Ce concentration, the Burstein–Moss shift which is a factor of increasing the band gap because evident and shouldn’t be neglected. As a result, the band gap of Ce@Si-T-III and Ce@Si-T-IV show slight increase, which is 3.122 eV and 2.973 eV, respectively. We can also see from the band structure that γ-Si_3N_4 has the direct band gap whose highest VB and lowest CB located at the same point. Among the four Ce@Si-T cases, only the Ce@Si-T-III has the character of direct band gap. With the reduced direct band gap, Ce@Si-T-III has the potential application in photodiode.

3.2.2. Electronic properties of Ce@Si-O cases

Considering that the doping methods of Ce@Si-O and Ce@Si-T has the similar E_b, the electronic structure of the high concentration cases deprived from Ce@Si-O are calculated and compared with those deprived from Ce@Si-T. For the same doping concentration, Ce@Si-O is more effective to decrease the band gap of γ-Si_3N_4 (Figure 5). Ce@Si-O-I has the direct band gap which is 2.440 eV, while that of Ce@Si-T-I is 4.069 eV. The composition of VB and CB of Ce@Si-O-I is similar to that of Ce@Si-T-I. However, the distribution of the orbitals and the band gap values are different from those of Ce@Si-T-I. This is because that the different doping method of Ce (Ce@Si-T or Ce@Si-O) causes the different interaction of electronic charges, then the overlap of impurities and defect band show different effects. It is noted that the band gap values of the Ce@Si-O case decrease continuously with the increase of doping concentration. This implies that the multi-body effect hold the dominant position in reducing the band gap value in the Ce@Si-O case. When the Ce concentration reaches 0.16, the Ce-5d orbitals of Ce@Si-O-IV move down to the Fermi energy and overlap with the VB. As a result, the band gap of Ce@Si-O-IV disappears, which shows that Ce@Si-O-IV is metallic. The changes of electronic properties will inevitably affect the optical properties.

3.3 Optical properties of doped γ-Si_3N_4

3.3.1. Imaginary part of dielectric function

Imaginary part of dielectric function constructs the bridge for understanding the relationship between electronic structure and interband transition. γ-Si_3N_4 is a direct and broad gap semiconductor whose spectrum is caused by electrons transition among energy level. Its dielectric peak and the corresponding optical properties can be explained by the DOS and band structure. [22] Figure 6 shows the imaginary part of dielectric function. An apparent dielectric peak locates at 11eV (L1), which originate from the transition between N-2p orbitals in VB and Si-3s orbitals in CB. Both the doping methods of Ce@Si-T and Ce@Si-O can result in the red shift of dielectric peak. Carefully checking Ce@Si-T-I and Ce@Si-O-I with the same concentration of 0.042, we find that there are some subtle differences between the two curves of dielectric function. Moreover, the difference between the curves of Ce@Si-T-II and Ce@Si-O-II and those of Ce@Si-T-III and Ce@Si-O-III become quite small, which show that doping methods play a small role in the electron transition below the doping concentration of 0.125. When the doping concentration reaches 0.167 (correspond to the cases of Ce@Si-T-IV and Ce@Si-O-IV), the difference of the two dielectric curves become obvious abruptly. Ce@Si-T-IV causes the relative higher dielectric peak at about 5.1 eV (L2). This implies that the doping method of Ce@Si-T under the concentration of 0.167 is effective. Combing the DOS and the band structure, one can find that the peak L2 of Ce@Si-T-IV origins from the direct transition at X point from N-2p orbitals at the highest VB to Ce-5d orbitals in CB (at about 4.6 eV). The lower energy electron transition may indicate the red shift of absorption edge.

3.3.2. Absorption coefficient and transmissivity

To widely understand the effect of the dopant and doping methods on γ-Si_3N_4, we calculated the absorption coefficient and transmissivity. Figure 7 shows the absorption coefficient of intrinsic γ-Si_3N_4 and Ce doped γ-Si_3N_4. The absorption edge of γ-Si_3N_4 is about 7.35 eV which is beyond the range of visible light. In the cases with Ce@Si-T method, the absorption edges appear gradual redshift with the increase of doping concentration. This trend is true for the cases with Ce@Si-O method. The redshift of the absorption edge can be explained by the enhanced interband transition in the low energy region as mentioned in the dielectric function analysis. Although both the doping methods are able to make the absorption edge of γ-Si_3N_4 occur redshift, the Ce@Si-T method is more effective when the concentration is beyond 0.042. This can be seen from the extended lines in Figure 7, which stand for absorption edges, that the absorption edge of the cases with Ce@Si-T method always locate in the lower energy than those with Ce@Si-O method, although the trend is not very obvious in the two cases with the concentration of 0.042. Ce@Si-T-IV whose absorption edge reduces by 2.27 eV compared with intrinsic γ-Si_3N_4 is the most effective doping case in reducing the absorption edge. However, the situation is different for the effect of increasing visible light absorption in the region from 1.5 to 3.5 eV. We can see from the inset in Figure 7 that when the concentration is 0.125, the absorption coefficient of Ce@Si-O-III is bigger than that of Ce@Si-T-III. Similarly, when the concentration reaches 0.167, the absorption coefficient of Ce@Si-O-IV is bigger than that of Ce@Si-T-IV. For the remaining cases with the lower concentration of 0.042 and 0.083, the trend is not clear. That is to say, Ce@Si-O is more effective to increase the visible light absorption when the concentration reaches 0.125. The absorption coefficient of Ce@Si-O-IV is enhanced significantly in the visible light region, which is up to $10^3 cm^{-1}$. Its enhancement of visible light absorption originates from the electron transition between the overlapped VB and CB. This indicates that Ce@Si-O-IV can absorb solar energy, which makes it be a potent candidate material of absorption device.

The transmissivity is also an important index to appreciate the optical properties of materials. The results for the considered Ce-doped systems are shown in Figure 8. The transmissivities of all Ce-doped cases change slightly in the low energy region (from 1.0eV to 3.0 eV). Ce doping reduced the transmissivity of intrinsic γ-Si_3N_4 in general. The influence of doping method on the transmissivity can be ignored in the concentration of 0.042, 0.083 and 0.125. But when the concentration reaches 0.167, the influence of doping method becomes obvious. Transmissivity of Ce@Si-T-IV falls below 0.8 while that of Ce@Si-O-IV maintains 0.85 above. On the whole, the transmissivity of Ce-doped cases are all above 0.75, which show a good transmittance. Combing the increase of light absorption coefficient and the good transmittance, the Ce-doped γ-Si_3N_4 can be used as potential window material of solar cell.

4. Conclusions

In summary, we investigate the influence of doping method and concentration on the electronic and optical properties of Ce doped γ-Si_3N_4. The doping method of Ce@Si-O is more effective to decrease the band gap than Ce@Si-T in the same doping concentration. The band gap values of Ce@Si-T-III and Ce@Si-O-I are 3.122

and 2.440 eV, respectively. The two cases with direct band gap can be used as promising LED material. The influence of doping method on the optical properties can be neglected below the concentration of 0.042. When the concentration reaches 0.167, the absorption edge of Ce@Si-T-IV reduces by 2.27 eV, and the absorption coefficient of Ce@Si-O-IV increases to 10^3 cm^{-1} in the region from 1.5 to 3.5 eV. This is caused by the enhanced electron transition in the low energy region. The combination of the enhanced absorption coefficient and the good transmittance in the range of solar light makes Ce-doped γ-Si_3N_4 a good window material that can be engineered to suit the desired application. The present results can provide helpful information for designing and preparing effective optical material based on Ce doped γ-Si_3N_4.

Acknowledgements

This work was supported by the National Science Foundation of China (Grant Nos. NSFC-11174117 and NSFC-11374132).

References

1 F. Oba, K. Tatsumi, I. Tanaka and H. Adachi, *J. Am. Ceram. Soc.*, 2002, **85**, 97-100.

2 F. Oba, K. Tatsumi, H. Adachi and I. Tanaka, *Appl. Phys. Lett.*, 2001, **78**, 1577-1579.

3 A. Zerr, M. Kempf, M. Schwarz, E. Kroke, M. Goken and R. Riedel, *J. Am. Ceram. Soc.*, 2002, **85** 86-90.

4 A. Zerr, G. Miehe, G. Serghiou, M. Schwarz, E. Kroke, R. Riedel, H. Fueß, P. Kroll and R. Boehler, *Nature,* 1999, **400**, 340-342.

5 T.D. Boyko, E. Bailey, A. Moewes and P.F. McMillan, *Phys. Rev. B,* 2010, **81**, 155207.

6 T.D. Boyko, A. Hunt, A. Zerr and A. Moewes, *Phys. Rev. Lett.*, 2013, **111**, 097402.

7 Y. Ding, H. Zhou, M. Xu, Y. Shen, Q. Chen, W.-j. Zhu and H. He, *Int. J. Mod. Phys. B*, 2008, **22**, 2157-2167.

8 Y.C. Ding, M. Xu, H.Z. Pan, Y.-B. Shen, W.-J. Zhu and H.-L. He, *Acta Phys. Sin.*, 2007, **56**, 117.

9 W. Ching and P. Rulis, *Phys. Rev. B*, 2006, **73**, 045202.

10 M. Xu, Y.C. Ding, G. Xiong, W.J. Zhu and H.L. He, *Physica B: Condens. Matter*, 2008, **403**, 2515-2520.

11 Y.C. Ding, A.P. Xiang, M. Xu and W.J. Zhu, *Physica B: Condens. Matter*, 2008, **403**, 2200-2206.

12 Y.C. Ding, A.P. Xiang, J. Luo, X.J. He, Q. Cai and X.F. Hu, *Physica B: Condens. Matter*, 2010, **405**, 828-833.

13 B. Huang, Y. Ma, S. Qian, D. Zou, G. Zheng and Z. Dai, *Optical Materials*, 2014, **36**, 1561-1565.

14 S.F. Wang, J. Zhang, D.W. Luo, F. Gu, D.Y. Tang, Z.L. Dong, G.E.B. Tan, W.X. Que, T.S. Zhang, S. Li and L.B. Kong, *Prog. Solid State Chem.*, 2013, **41**, 20-54.

15 J. Ruan, R.-J. Xie, S. Funahashi, Y. Tanaka, T. Takeda, T. Suehiro, N. Hirosaki and Y.-Q. Li, *J. Solid State Chem.*, 2013, **208**, 50-57.

16 X. Wang, G. Zhou, H. Zhang, H. Li, Z. Zhang and Z. Sun, *J. Alloys Compd.*, 2012, **519**, 149-155.

17 M. Sopicka-Lizer, D. Michalik, J. Plewa, T. Juestel, H. Winkler and T. Pawlik, *J. Eur. Ceram. Soc.*, 2012, **32**, 1383-1387.

18 H. Yang, Y. Liu, S. Ye and J. Qiu, *Chem. Phys. Lett.*, 2008, **451**, 218-221.

19 Y.Q. Li, N. Hirosaki, R.J. Xie, T. Takeda and M. Mitomo, *J. Lumin.*, 2010, **130**, 1147-1153.

20 S. Clark, M. Segall, C. Pickard, P. Hasnip, M. Probert, K. Refson and M. Payne, *Z. Kristallogr*, 2005, **220**, 567-569.

21 Y.-X. Han, C.-L. Yang, Y.-T. Sun, M.-S. Wang and X.-G. Ma, *J. Alloys Compd.*, 2014, **585**, 503-509.

22 Y.-X. Han, C.-L. Yang, J.-S. Yang, M.-S. Wang and X.-G. Ma, *Physica B: Condens. Matter*, 2013, **417**, 17-23.

Table 1. Calculated E_fs, E_bs and structural properties for different doping structures. E_f _Si is calculated from Si-rich limit while E_f _N from N-rich limit.

	E_f_Si(eV)	E_f_N(eV)	E_b(eV)	N–Si (avg) (Å)	Lattice parameter (Å)
γ-Si_3N_4	0.613	0.613	-455.034	1.862	7.771,7.745[a], 7.837[b]
Ce@Si-T	-3.103	-6.224	-453.398	1.875	7.871
Ce@Si-O	-0.751	-3.872	-451.046	1.875	7.875
Ce@N	29.095	31.435	-416.328	1.862	7.778
Ce-IN	6.583	6.583	-449.065	1.895	7.926

[a] Ref. 7

[b] Ref. 9

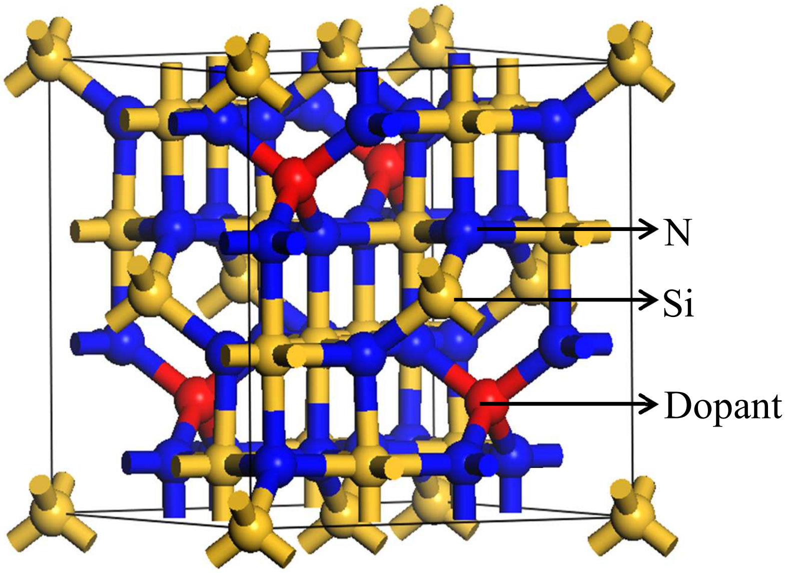

Figure 1. Model of doped γ-Si_3N_4.

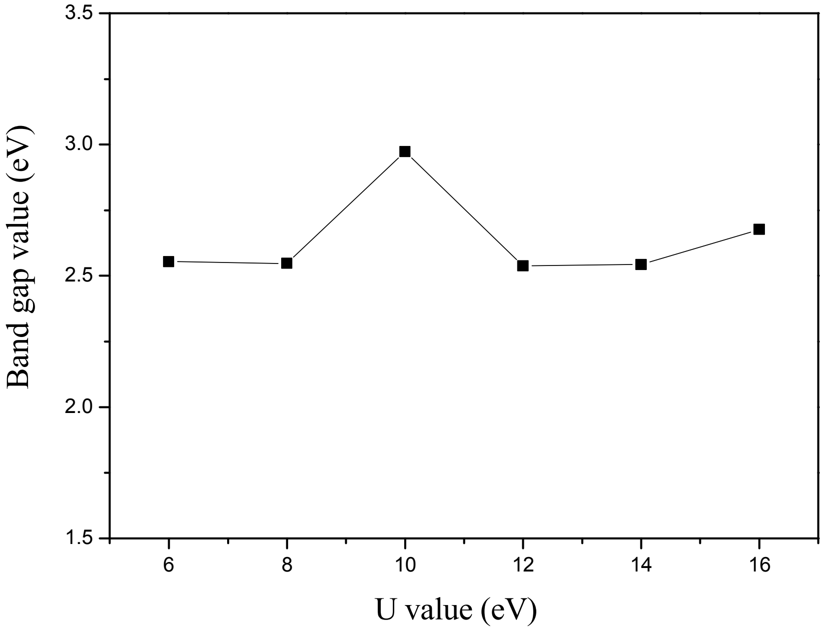

Figure 2. The value of U verses band gap value.

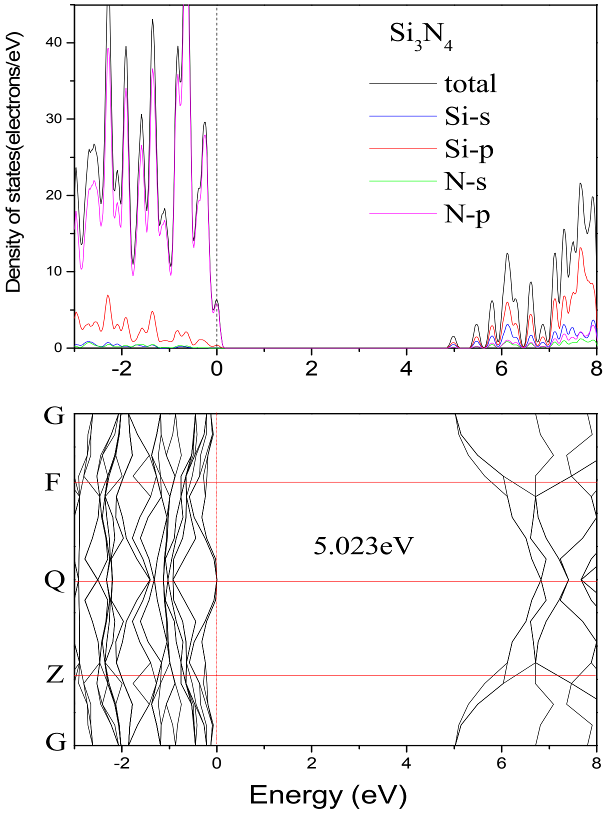

Figure 3. Density of states and band structure for intrinsic γ-Si_3N_4.

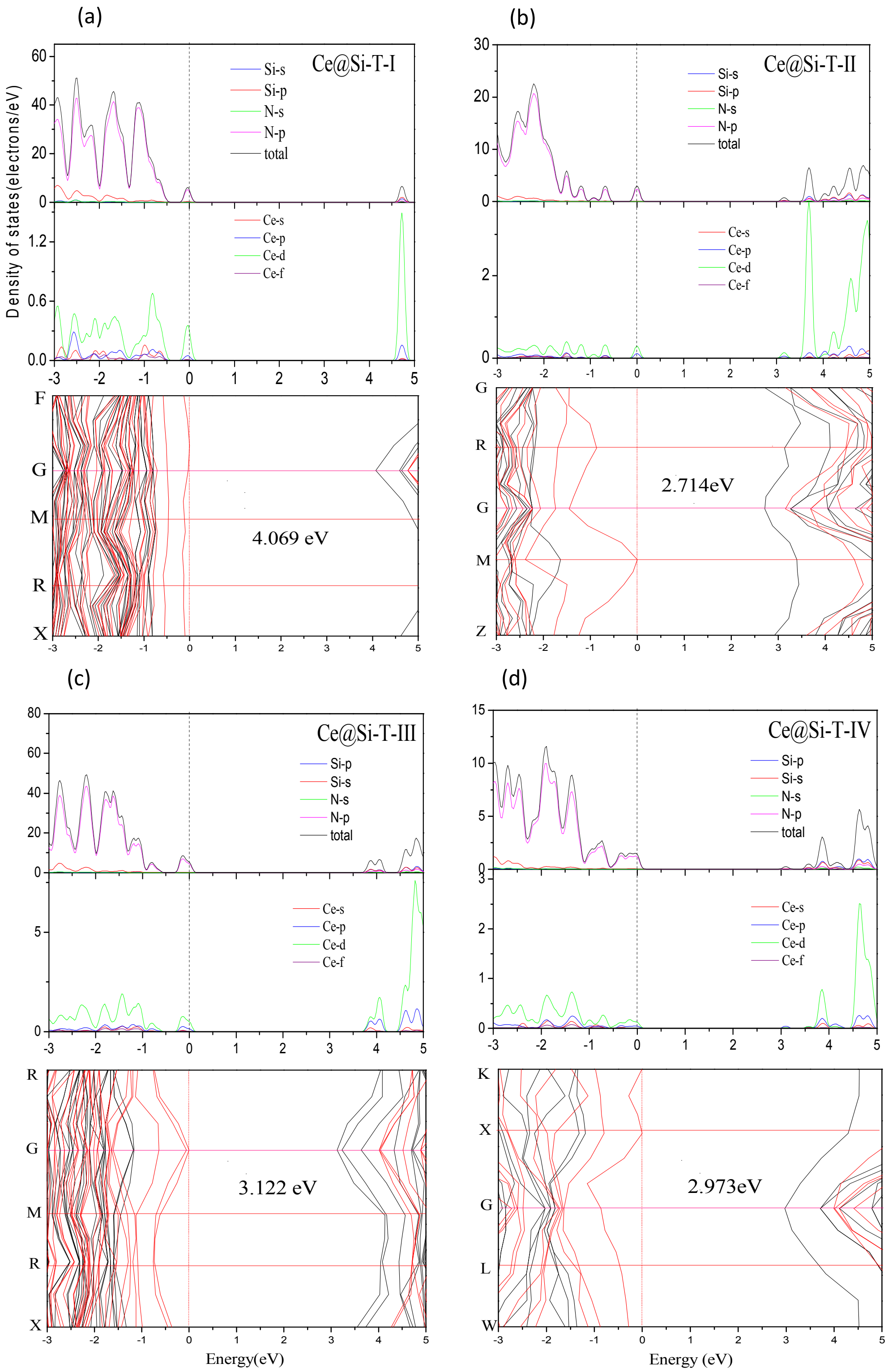

Figure 4. Density of states and band structure for Ce@Si-T cases.

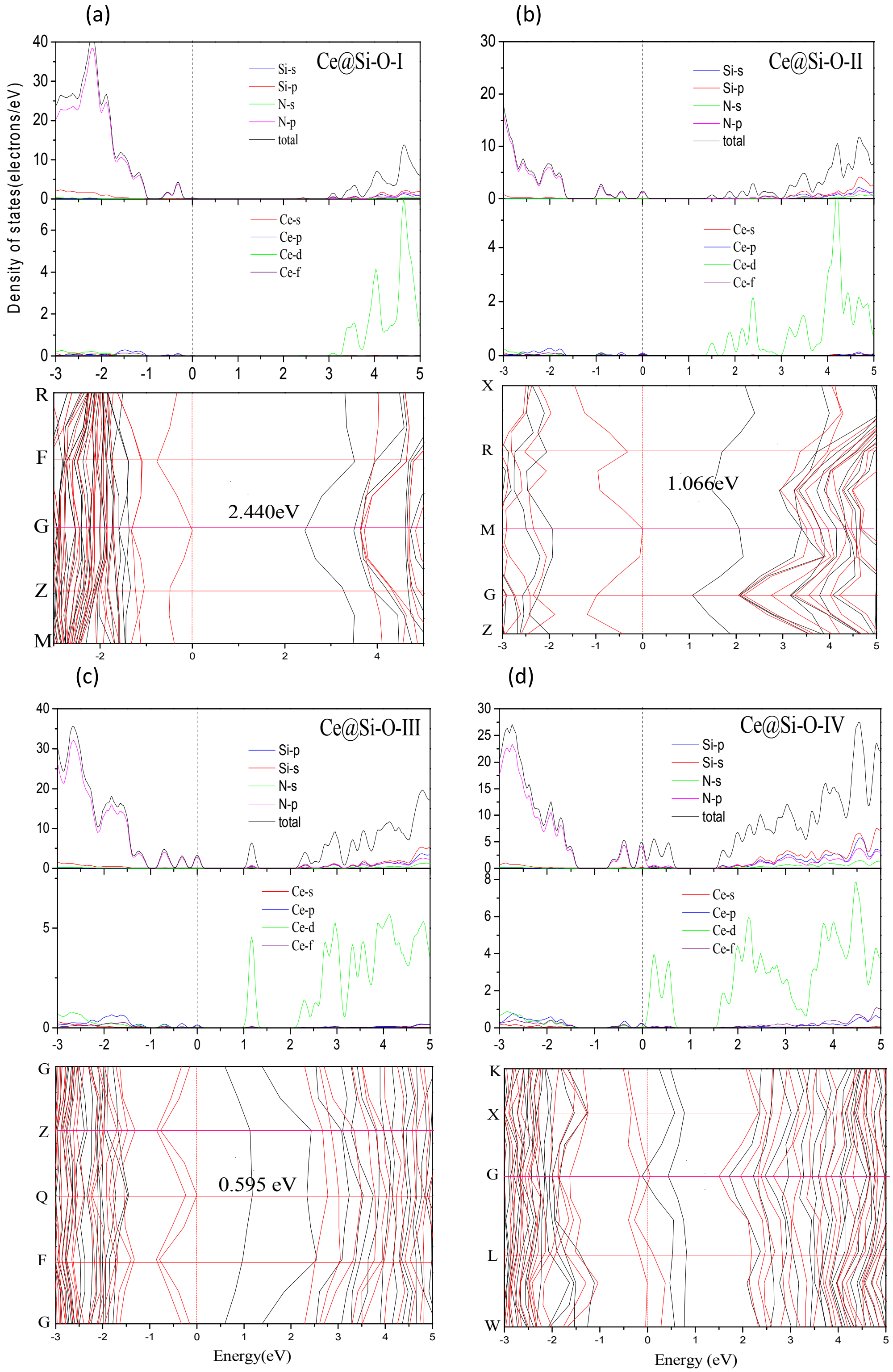

Figure 5. Density of states and band structure for Ce@Si-O cases.

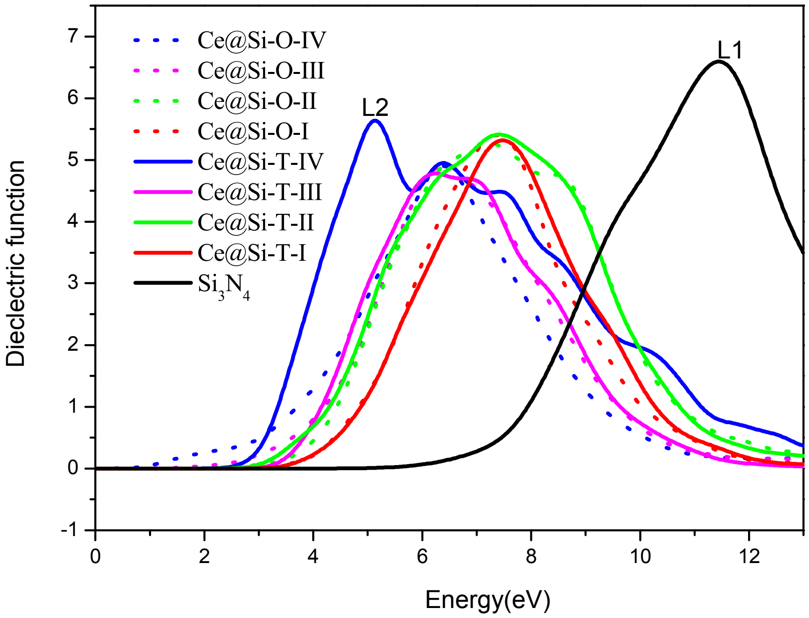

Figure 6. Dielectric function for intrinsic and Ce doped γ-Si_3N_4.

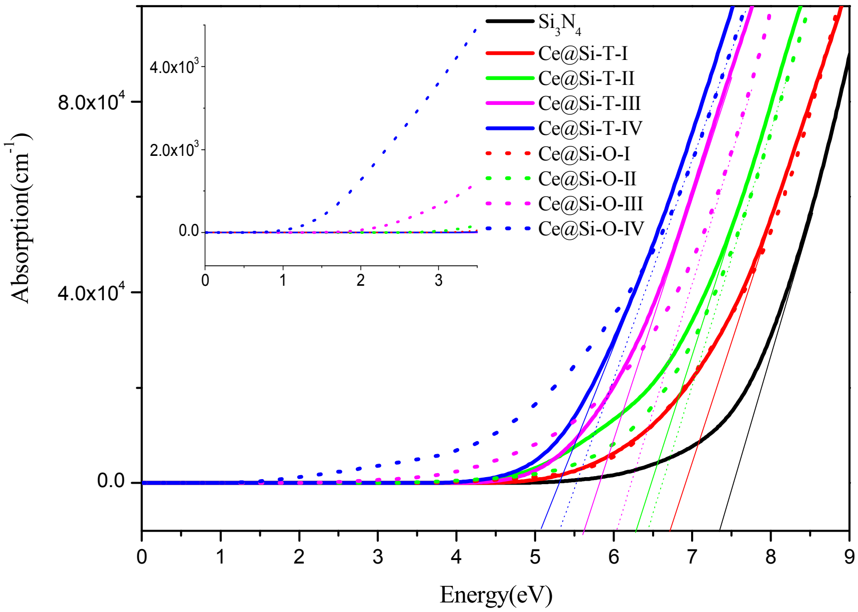

Figure 7. Absorption coefficient for intrinsic and Ce doped γ-Si_3N_4.

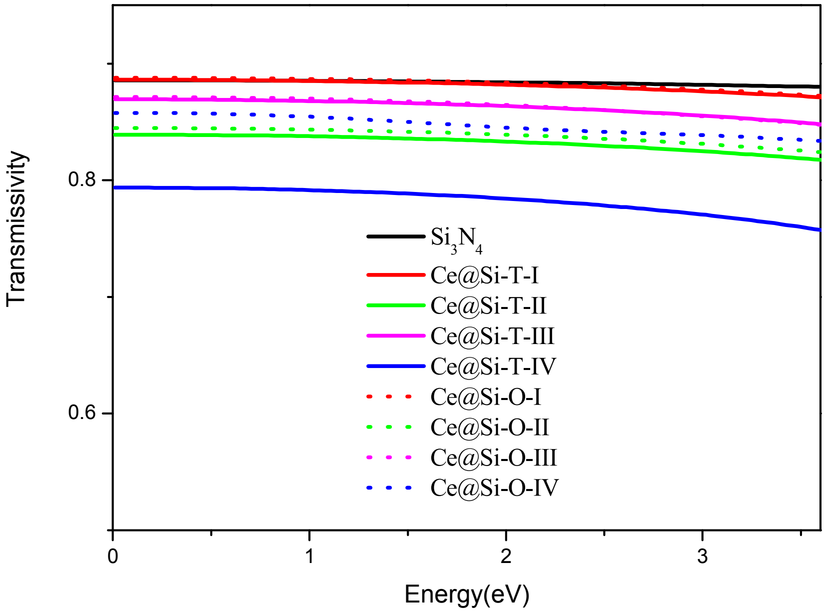

Figure 8. Transmissivity for intrinsic and Ce doped γ-Si_3N_4.